Neurobiology of Aging 94 (2020) 217–226

Contents lists available at ScienceDirect

Neurobiology of Aging

journal homepage: www.elsevier.com/locate/neuaging

# Forecasting memory function in aging: pattern-completion ability and hippocampal activity relate to visuospatial functioning over 25 years

Lars Nyberg[a,b,c,d,*], Xenia Grande[e,f], Micael Andersson[b,c], David Berron[e,f,g], Anders Lundquist[c,h], Mikael Stiernstedt[b,c], Anders Fjell[d], Kristine Walhovd[d], Greger Orädd[a,c]

[a] Department of Radiation Sciences, Umeå University, Umeå, Sweden
[b] Department of Integrative Medical Biology, Umeå University, Umeå, Sweden
[c] Umeå Center for Functional Brain Imaging (UFBI), Umeå University, Umeå, Sweden
[d] UiO Center for Lifespan Changes in Brain and Cognition, Department of Psychology, University of Oslo, Oslo, Norway
[e] German Center for Neurodegenerative Diseases (DZNE), Magdeburg, Germany
[f] Institute of Cognitive Neurology and Dementia Research, Otto-von-Guericke University Magdeburg, Magdeburg, Germany
[g] Clinical Memory Research Unit, Department of Clinical Sciences Malmö, Lund University, Lund, Sweden
[h] Department of Statistics, USBE Umeå University, Umeå, Sweden

ARTICLE INFO

*Article history:*
Received 10 December 2019
Received in revised form 1 June 2020
Accepted 5 June 2020
Available online 12 June 2020

*Keywords:*
Episodic memory
General cognitive function
Hippocampus
Subfields

ABSTRACT

Heterogeneity in episodic memory functioning in aging was assessed with a pattern-completion functional magnetic resonance imaging task that required reactivation of well-consolidated face-name memory traces from fragmented (partial) or morphed (noisy) face cues. About half of the examined individuals ($N = 101$) showed impaired (chance) performance on fragmented faces despite intact performance on complete and morphed faces, and they did not show a pattern-completion response in hippocampus or the examined subfields (CA1, CA23, DGCA4). This apparent pattern-completion deficit could not be explained by differential hippocampal atrophy. Instead, the impaired group displayed lower cortical volumes, accelerated reduction in mini-mental state examination scores, and lower general cognitive function as defined by longitudinal measures of visuospatial functioning and speed-of-processing. In the full sample, inter-individual differences in visuospatial functioning predicted performance on fragmented faces and hippocampal CA23 subfield activity over 25 years. These findings suggest that visuospatial functioning in middle age can forecast pattern-completion deficits in aging.


## 1. Introduction

Individual differences in how episodic memory (EM) changes with advancing age are well documented (Josefsson et al., 2012; Lindenberger, 2014; Nyberg and Pudas, 2019). It is also well established that the magnitude of age-related impairment varies depending on the nature of testing conditions. One fundamental dimension is the degree of cue completeness. In many experimental and everyday situations, an original memory trace is reactivated based on cue information entailing only parts of the original memory—a computation referred to as *pattern completion* (Marr, 1971; McClelland et al., 1995). Past studies indicate that the age-related EM deficit becomes magnified as a function of reduced cue completeness (Paleja and Spaniol, 2013; Vieweg et al., 2015), which is suggestive of a pattern-completion deficit in aging. Thus, although the evidence is still limited, it may be that tasks taxing pattern completion are particularly sensitive for revealing heterogeneity in EM functioning in older populations.

The mechanisms underlying a pattern-completion deficit in aging remain unclear. Pattern completion has since long been associated with the hippocampus (HC), in particular the CA3 subfield (Marr, 1971; see, e.g., Hunsaker and Kesner, 2013). Findings from rodent studies (Neunuebel and Knierim, 2014) and human 7T MRI (Grande et al., 2019) support a role of CA3 in pattern completion. There is evidence that most older adults, even those at low risk for neurodegenerative disease, display some changes in hippocampal regions (Fjell et al., 2013, 2014). A dominating theory is that

* Corresponding author at: Department of Radiation Sciences, Umeå University, Umeå 90197, Sweden. Tel.: +46-90-7866429; fax: +46-90-7866696.
*E-mail address:* lars.nyberg@umu.se (L. Nyberg).

0197-4580/
https://doi.org/10.1016/j.neurobiolaging.2020.06.005

variable rates of hippocampal atrophy and functional responsiveness account for EM heterogeneity in aging (Buckner, 2004; Nyberg et al., 2012; Nyberg and Lindenberger, 2020), suggesting that age-related hippocampal atrophy, notably in CA3, may explain impaired pattern-completion ability in aging.

Another reason why pattern-completion tasks may be particularly age-sensitive is that reducing cue completeness confers increased demands on several cognitive processes (Honey et al., 2017; Marr, 1971; Tang et al., 2018). Those processes include but are not limited to sustained attention, visuospatial processes, executive hypothesis testing operations, and other fluid cognitive functions that jointly have been referred to as *general (fluid) cognitive function*, GCF (Davies et al., 2015). There is evidence for a strong GCF-EM association that can be described as a hierarchical GCF to EM relation (Deary et al., 2010; Salthouse, 2004). By this view, individuals with higher GCF functions tend to score higher on EM tasks. Longitudinal investigations have revealed long-term stability of individual differences in GCF (Arbuckle et al., 1998; Gow et al., 2011; Kremen et al., 2019; Rönnlund et al., 2015; Walhovd et al., 2016). Moreover, there is strong evidence from twin (McClearn et al., 1997) and genome-wide association (Davies et al., 2015) studies for genetic effects on GCF in middle and older age. Thus, a major predictive factor of impaired pattern-completion ability in aging could be "lifelong" lower GCF.

Here, taking advantage of one of the longest existing longitudinal datasets on neurocognitive function, the Betula study (Nilsson et al., 2004), we related pattern-completion performance and associated hippocampal-functional activity to longitudinal patterns of hippocampal and cortical structural integrity and to GCF. Pattern completion was assessed at the latest wave of the Betula study (Wave 7; Fig. 1A) using a new functional magnetic resonance imaging (fMRI) task (Fig. 1B). This task was built on a face-name fMRI task that was included at Waves 5–7, but it was unconfounded by practice effects. Specifically, consistent with the definition of pattern completion, the new task required reactivation of well-consolidated face-name memory traces from partial (fragmented) or noisy (morphed) face cues. Both partial and noisy cues can trigger pattern completion (Hunsaker and Kesner, 2013; Liu et al., 2016), but fragmented faces are more process pure than morphed faces, for which both correct old and "new" responses are formally correct and hence could tap other mnemonic processes as well (Hunsaker and Kesner, 2013). We therefore categorized the

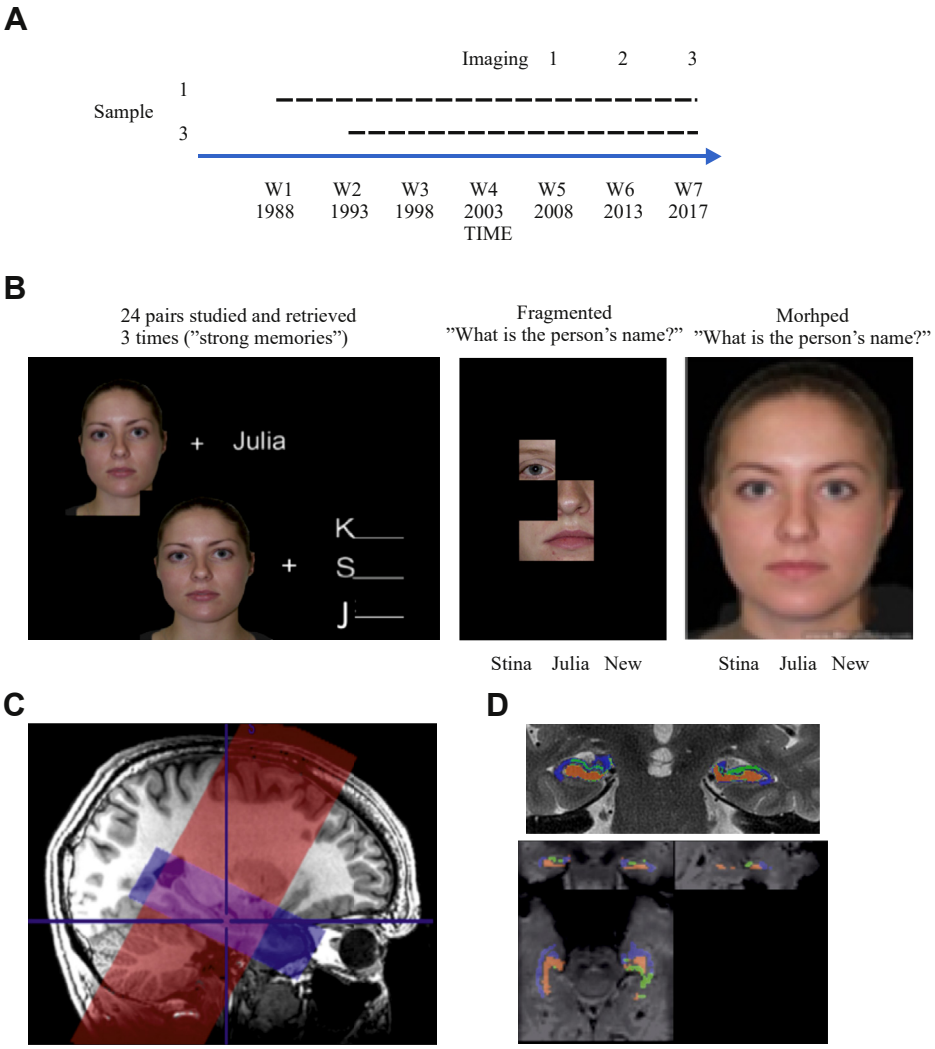


**Fig. 1.** (A) Outline of the longitudinal design with 7 test waves (W1–7) and 3 imaging waves. (B) The face-name task and examples of fragmented and morphed face cues. (C) The scanned areas in the high-resolution MRI sessions. The red and blue contours indicate the HR-T2w and the functional volumes, respectively. (D) Hippocampus subfields (from FreeSurfer), colored as blue (CA1), green (CA23), and orange (DGCA4), overlayed on HR-T2w-image (top) and functional image (bottom). Key: HR-T2w, T2-weighted data; MRI, magnetic resonance imaging.

participants as pattern-completion "intact" or "impaired" based on their performance on fragmented cues.

The pattern-completion intact and impaired groups were compared on hippocampal subfield (Fig. 1C and D) functional activity, and also HC atrophy and cortical gray matter (GM) volume change (3 repeated measures over 10 years). Building on previous work (Deary et al., 2010; Duncan, 2013; Jung and Haier, 2007; Salthouse, 2004), particular focus was on frontal and parietal cortical gray matter (GM) volume. The intact and impaired groups were also compared on 6 repeated test waves of GCF and mini-mental state examination (MMSE) (Folstein et al., 1975), spanning 25 years. In previous work (Davies et al., 2015), we defined GCF based on visuospatial functioning (block design), speeded task performance (letter digit substitution, fluency), and EM (verbal recall). Here, when pattern completion was the outcome, we omitted EM measures from the GCF composite and used block design and letter digit substitution (in combination and separately) as indicators of GCF. Continuous regression analyses of the entire sample were conducted to identify the strongest predictors of heterogeneity in pattern-completion ability and functional activity in the HC and its subfields.

## 2. Materials and methods

### 2.1. Participants

The participants in the present study were from the longitudinal Betula study on memory, health, and aging. The research was approved by the local ethics board at Umeå University, Sweden. All participants provided written informed consent and were compensated monetarily for their participation. The samples, recruitment procedure, offline procedures, imaging procedures, and other methodological details have been described in detail in several prior publications (Nyberg et al., 2019; Pudas et al., 2018). Here we focus on materials and methods of relevance to this study.

The participants in this study were from the 2 main longitudinal samples of approximately 1000 participants each, included at the first (Sample 1) or second (Sample 3) Betula test wave (Fig. 1A). At Wave 5, 292 of these participants were part of a larger imaging study, 177 were rescanned at Wave 6 (for a drop-out analysis, see Nyberg et al., 2019), and 101 at Wave 7 (Table 1). Thus, 3 test waves were of particular importance: Wave 2, when all participants underwent cognitive testing; Wave 5 being the first with imaging data; and Wave 7—the final test wave for both cognition and imaging—that served as outcome.

### 2.2. Offline cognitive testing

The MMSE task was administered at each test wave (maximum = 30). Data from tests of visuospatial ability (block design) and speed of processing (letter digit substitution) were used to define a composite measure of GCF (Davies et al., 2015). The maximum score of the composite task was 176, except for Wave 2 when the speed task was not included (maximum = 51). To investigate the change over time and groups, we used repeated measures analysis of covariance with age at baseline as a covariate to adjust for age differences between groups. We used this for all individual tests as well as the composite measure. In order to make the composite score comparable across all time points, we standardized, by *z*-transformation, each test with respect to its mean and standard deviation at the third test wave (i.e., the wave at which the speed test was introduced). For Waves 3–7 respectively, we added the standardized scores to obtain a composite score. For Wave 2, where the speed test was not available, the standardized Block Design score was multiplied by 2 to ensure comparability with composite scores from Waves 3–7. Finally, we characterize the groups in terms of their offline performance on several measures of EM that formed an EM composite score (Table 1).

### 2.3. fMRI task

A face-name paired associates task was included at all 3 imaging waves (Nyberg et al., 2019). This 10-minute task comprised 6 blocks of face-name encoding (remember a name associated with a face), 6 blocks of cued-name retrieval (indicate the first letter corresponding to the name previously encoded with a face), and 8 blocks of an active control task involving a simple perceptual discrimination (pressing a button each time a fixation mark changed into a circle). Scanner task performance was calculated as mean number (%) of correct answers. A novel fMRI task was added for at the third MRI wave (Betula Wave 7; Fig. 1A). It was a 12-minute task containing a total of 62 cued-name retrieval items. These items were made up of altered versions of faces that had been previously presented during the face-name task, as well as faces that had not been presented before. Three different kinds of items were presented during this test: fragmented images (24 old + 4 new faces), noisy images (24 old + 4 new faces), and unaltered images (6) that previously were presented during the face-name task. The fragmented images were made by covering the images in black, then, by revealing the face via 4 squares showing approximately 20%–25% of the face. The squares were placed so that at least the mouth, nose, and one of the eyes were shown on all faces. The fMRI task also included a condition with *noisy* cues, made up by morphing (50–50) each original face with a unique new face. Each morphing pair was matched on gender, approximate size of the face and hair so that there would be less artifacts from the morphing. Base morphing of the faces was done via www.morphthing.com; images were cleaned from major artifacts in an image editing software. Presentation order was randomized for all participants. Each item was presented for a total of 6 seconds, the 3 possible answers that

**Table 1**
Sample characteristics

| | Whole sample[a] | Intact group | Impaired group | Age matched intact group | Age matched impaired group |
|---|---|---|---|---|---|
| Women | $N = 44$ | $N = 21$ | $N = 21$ | $N = 14$ | $N = 12$ |
| Men | $N = 57$ | $N = 29$ | $N = 26$ | $N = 20$ | $N = 22$ |
| Age (y) | 72.3 | 69.7 | 74.9 | 72.6 | 72.6 |
| Age range (y) | 63.0–87.9 | 63.0–82.5 | 63.4–87.9 | 64.0–82.5 | 63.4–84.3 |
| Education (y | 13.8 | 14.3 | 13.6 | 13.4 | 14.2 |
| APOE-4 carriers | $N = 33$ | $N = 14$ | $N = 19$ | $N = 6$ | $N = 16$ |
| Episodic memoryMean score[b] | 11.1 | 11.9 | 10.3 | 11.0 | 10.8 |

[a] Note: 101 participants were scanned at Wave 7, but some had to be excluded in certain analyses as detailed in the text.
[b] Maximum score for the EM composite = 28. The difference between the intact and impaired groups was significant before [$t(95) = 2.43$, $p = 0.017$, 2-sided] but not after [$t(66) = 0.24$, $p = 0.807$, 2-sided] age matching the groups.

the participant could choose from, that is, the name of the shown face, another name that previously had been paired with another face, and "new," were shown during the last 4 seconds (Fig. 1B). The inter-stimulus interval (ISI) was randomly jittered among 2.5 (21 ISIs), 5 (21 ISIs), or 7.5s (20 ISIs) during which a cross hair (+) was displayed. Responses were given through a button press on a scanner-compatible response pad, and participants were instructed to guess if uncertain. All participants completed a short practice version of the task at least once prior to scanning. In the scanner room, the task was displayed on a computer screen seen through a tilted mirror on the head coil. Old hit rate is defined as responding to an old face (fragmented or morphed) with the correct old name (rather than choosing the incorrect old name or "new").

### 2.4. fMRI acquisition

The same 3T General Electric scanner (equipped with a 32-channel head coil) was used to collect images at all imaging sessions. Functional images for the complete face-name task were acquired with a gradient echoplanar imaging sequence (37 transaxial slices; thickness: 3.4 mm, gap: 0.5 mm, repetition time (TR): 2000 ms, echo time (TE): 30 ms, flip angle: 80°, field of view: 25 × 25 cm, matrix: 96 × 96 voxels [zero-filled to 128 × 128]). High-resolution functional MRI images (HR-fMRI), with an isotropic resolution of 1.5 mm, were acquired with a reduced field-of-view on the mid part of the brain with an echoplanar imaging sequence (20 slices oriented parallel to the long axes of the left and right HC; thickness: 1.5 mm, no gap, TR: 1500 ms, TE: 30 ms, flip angle: 75°, field of view: 9.6 × 9.6 cm, matrix: 64 × 64) with 10 dummy scans collected and discarded before the collection of 470 volumes. Total acquisition time was 11 minutes, 45 seconds.

### 2.5. Additional MRI scans

T1-weighted data (T1w) were acquired in axial orientation with a 3-dimensional fast spoiled gradient echo sequence (180 slices with 1 mm thickness, TR: 8.2 ms, TE: 3.2 ms, TI: 450 ms, flip angle: 12°, field of view: 25 × 25 cm, matrix: 256 × 256, reconstructed to 512 × 512). For the HR T2-weighted data (HR-T2w) a PROPELLER sequence was employed with high in-plane resolution and the slices covering the HC in a perpendicular orientation with respect to the HC long axis (TR: 5925 ms, TE: 92.344 ms, echo train length: 28, flip angle: 120°, number of excitations: 2.5, 31 slices of 2.0 mm thickness and no gap, field of view: 20.48 cm, matrix 512 × 512, resulting in an in-plane resolution of 0.4 mm). The B0 field was collected with a fast gradient echo sequence (B0-map). The sequence produced magnitude images which were coregistered with the T1w image, and B0-maps which were transformed to T1w space using the same transformation matrix.

### 2.6. VBM analyses

For the voxel-based morphometry (VBM) analyses, T1w images for each participant and time point were segmented into GM, white matter, and cerebrospinal fluid likelihood maps in native (used for VBM) and DARTEL imported space (used for spatial normalization). For each individual, the DARTEL imported space files were processed in the DARTEL toolbox (Ashburner, 2007) of statistical parametric mapping (SPM) to make a participant-specific template and native → participant-template flow-field files were achieved. Next, the participants' templates were, in the same way, processed to make a group template and flow-field maps from participant-template → group-template were achieved. The GM files were normalized to Montreal Neurological Institute space with the flow-field maps by mapping native→participant-template→group-template and then by an affine transformation to Montreal Neurological Institute space. The signal amount was preserved during normalization (=modulated) and the images were smoothed by convolving with a Gaussian 6-mm filter. The files were mapped into 1-mm isotropic resolution. At each wave a 2-sample *t*-test was performed with the age-matched intact ($N = 34$) and impaired ($N = 33$) groups. ANCOVA regressors were added to the model and an explicit mask of areas from a mean T1w image with a GM likelihood larger than 0.2 was used. The core VBM results remained unchanged when using an explicit mask of GM >0.5 (i.e., all the clusters and selected peak coordinates remained unchanged, data not shown). A conjunction of the intact-impaired *t*-tests over the 3 waves was made with an uncorrected *p*-value threshold of 0.001 and an extent threshold of 80 voxels (80 $mm^3$). All preprocessing was performed with SPM12 functions.

### 2.7. Hippocampus subfield segmentation

Hippocampal subfield segmentation was performed with the HippocampalSubfield module of FreeSurfer v.6.0 (https://surfer.nmr.mgh.harvard.edu/fswiki/HippocampalSubfields). For the Wave 7 analyses, both T1w and HR-T2w structural images were used as input to the segmentation, while for the longitudinal analysis (Waves 5–7) only T1w images were used as input into the longitudinal stream (Reuter et al., 2012) in FreeSurfer. As a control analysis for the functional analysis, hippocampal subfield segmentation was performed with the Automatic Segmentation of Hippocampal Subfields (ASHS 1.0.0; Yushkevich et al., 2015) using an atlas developed to consider individual anatomical variability (Berron et al., 2017). Some of the participants were excluded due to problems with the segmentations. This resulted in a total of 98 participants remaining for the Freesurfer segmentation and 93 participants for the ASHS segmentation. For the age-matched groups (originally 34/group), the remaining number of participants in the intact/impaired group was 33/32 for Freesurfer and 32/30 for ASHS.

### 2.8. Comparison of volumes from subfield segmentations using T1w or T1w + T2w

The longitudinal subfield analysis could only use a T1w image as input, since the HR-T2w protocol was only included in Wave 7. A comparison was made on Wave 7 data between using only T1w and using both T1w and T2w images in the segmentation. Overall, agreement between the 2 methods was good with correlation coefficients above 0.95 and slopes between 0.88 and 1.05 for all subfields (CA1, CA2/3, DGCA4) and the whole HC (Fig. S1).

### 2.9. Preprocessing of the HR-fMRI data

The data were corrected for slice timing and head movement, and they were corrected for B0 field inhomogeneities using the measured B0-map. It proved to be difficult to register the functional data to T1w space using coregistering routines, due to the reduced field of view, poor contrast, and signal dropout in the functional images. Therefore, a different procedure was chosen as follows: first, the HR-T2w images were coregistered to T1w space. This was done in the FreeSurfer segmentation. The functional data were then coregistered using the transformation matrix for the HR-T2w → T1w coregistration. Since the functional scan was started within 30–60 seconds after the finish of the HR-T2w scan it was assumed that the participant had not moved between these 2 data collections, thereby making it possible to use this procedure. This assumption is believed to be accurate within 1.5 mm (1 voxel size), based on an analysis of the motion parameters from the functional

scan, where the mean displacements over all participants were 0.49 mm, with a standard deviation of 0.19 mm. Only 5 participants showed a displacement larger than 2 mm at any time during the 12-minute long functional scan. We cannot, however, exclude the possibility that some participants made substantial movements between the HR-T2w scan and the functional scan.

The voxel intensities were averaged over each subfield, using masks from the FreeSurfer T1w + T2w subfield segmentation, or from the ASHS segmentation, creating a single time series for each subfield. Since the definition of the subfields differ between the 2 methods, it is difficult to make direct comparisons. A subset of subfields was therefore selected that are most similarly labeled in both methods; CA1 (same label in both methods), CA2/3 (single label in FreeSurfer, 2 labels in ASHS), and DG/CA4 (2 labels in FreeSurfer, single label in ASHS). Despite this effort, there are still differences in the way these subfields are defined in each method, so one cannot expect the results to be exactly comparable.

### 2.10. Statistical analyses for the HR-fMRI

The time series for each subfield was analyzed in a general linear model for each participant. The events were modeled as a boxcar with the length of 3 TRs, convolved with the standard hemodynamic response function and initiated at stimulus onset (when each face was shown). The regressors based on the answers to the stimuli were as follows: frag_corr, frag_incorr, morph_corr, morph_incorr, where "corr" refers to answering the correct old name and "incorr" refers to selecting any of the other 2 choices (incorrect name or "new"). Four regressors of no interest—frag_new-face, morph_new-face, unaltered face, and hair-cross—were also included. In addition, 6 realignment parameters from the motion correction step and a second-order polynomial were included. The obtained beta values were used to create the contrasts and mean values and standard errors were calculated.

### 2.11. Statistical methods

The first set of main analyses was based on comparing the "Intact" and "Impaired" groups. They were defined using the hit rate for old faces in the fragmented faces task, where we considered performance at or below chance level indicative of impairment (see also Section 3.1). For comparing functional hippocampal responses as well as subfield and cortical volumes, we age-matched the groups since the impaired group turned out to be older on average. In analyses involving GCF (results presented in Section 3.5), we retained the whole groups and used age as a covariate in the models. This was done since preliminary analyses indicated residual age-confounding even after matching. Cross-sectional analyses were performed using 1- and 2-sample *t*-tests, Wilcoxon signed rank tests, Pearson correlation, or linear regression, while the longitudinal analyses were performed using repeated measures analysis of covariance. In the regression analyses, when possible, we considered a combined GCF score based on block design and letter-digit, as well as treating them as separate predictors.

### 2.12. Preprocessing and analyses of fMRI data

For each participant and time point, fMRI data during the complete face-name task were movement corrected and coregistered to the T1w image. The normalization procedure is similar to the VBM normalization described in Section 2.6 with the exception that the BOLD-signal-concentration was preserved during the normalization steps, and mapped into 2-mm isotropic resolution. The data were convolved with an 8-mm full width at half maximum Gaussian function. A map of B0-inhomogenities was recorded at Wave 7, which was used for adjustment of fMRI data. A boxcar model with regressors for encoding, retrieval, and baseline task was setup together with the 6 movement parameters achieved during the movement correction as nuisance regressors. The boxcar functions were convolved with the canonical hemodynamic response function in SPM. A linear regressor model was run in each voxel and a contrast between the achieved beta values for retrieval and baseline was stored and used. All steps except B0-inhomogenity adjustment were performed in SPM12. Batches of analyses were simplified by an in-house program DataZ.

## 3. Results

### 3.1. Heterogeneity in pattern-completion ability in aging

A sizable proportion of individuals in the sample performed at or below the chance level (33%) on the fragmented faces task. This proportion increased as a function of age (Fig. 2A), but a plot of scores confirmed heterogeneity in all age groups (Fig. 2B). In subsequent analyses, based on their old hit rate on the fragmented faces task (intact, range = 10–18; impaired, range = 4–9), the sample was split into "intact" ($N = 50$) and "impaired" ("at-chance," $N = 47$) pattern-completion groups. Level of education and the proportion of ApoE-ε4 carriers did not differ significantly between groups ($p$'s $> 0.40$; Table 1). To control for the higher mean age in the impaired group, age-adjusted analyses were conducted by age-matching the groups ($M = 72.6$ years, $N = 34$/group) or by including age as a covariate in the continuous analyses (3.5).

The Wave 7 performance on the complete face-name task was positively correlated with the probability of responding with the correct old name to fragmented faces ($r = 0.41$, $p = 0.000031$, $N = 97$), suggesting that the strength of face-name memory traces influenced pattern completion (correlation for the age-matched sample; $r = 0.29$, $p = 0.017$, $N = 68$). In the complete sample, the pattern-completion intact group showed significantly higher performance on complete faces [$t(95) = 3.16$, $p = 0.0011$ (one-sided)] and also on the EM composite (Table 1). After age matching, consistent with a pattern-completion deficit, the group difference remained on the fragmented faces ($p < 0.001$), whereas the performance for complete faces (across waves) and morphed faces at Wave 7 were comparable in the intact and impaired groups ($p$'s $>$ 0.05; Fig. 2C). A nonsignificant group difference was also seen for the EM composite after age matching (Table 1).

### 3.2. Hippocampal functional responses

To isolate a *pattern-completion signature*, that is, activation changes when an original memory trace was restored on basis of partial input, an fMRI contrast was set-up between fragmented old faces completed with the correct (old name) versus incorrect (new or incorrect old name) responses. In the entire sample ($N_{OBS} = 97$), a significant pattern-completion response (correct > incorrect) was observed in the whole HC as well as in all subfields (Fig. 3A). Group-specific analyses revealed a pattern-completion response across the *FreeSurfer*-segmented subfields in the intact group, whereas the response was weak and nonsignificant in the impaired group (Fig. 3B). Parametric and nonparametric statistical details are presented in Table S1. In a corresponding ASHS control analysis (Fig. S2a, see Methods), a similar pattern was seen with a pattern-completion response across subfields in the intact group (significant only for CA1), along with generally weaker responses in the impaired group (Fig. S2b).

The fMRI analysis of data from the morphed faces condition (old > new/other; Fig. 3C) revealed a similar BOLD-signal response pattern as for fragmented faces. Thus, older individuals with impaired pattern-completion ability on fragmented face cues showed altered

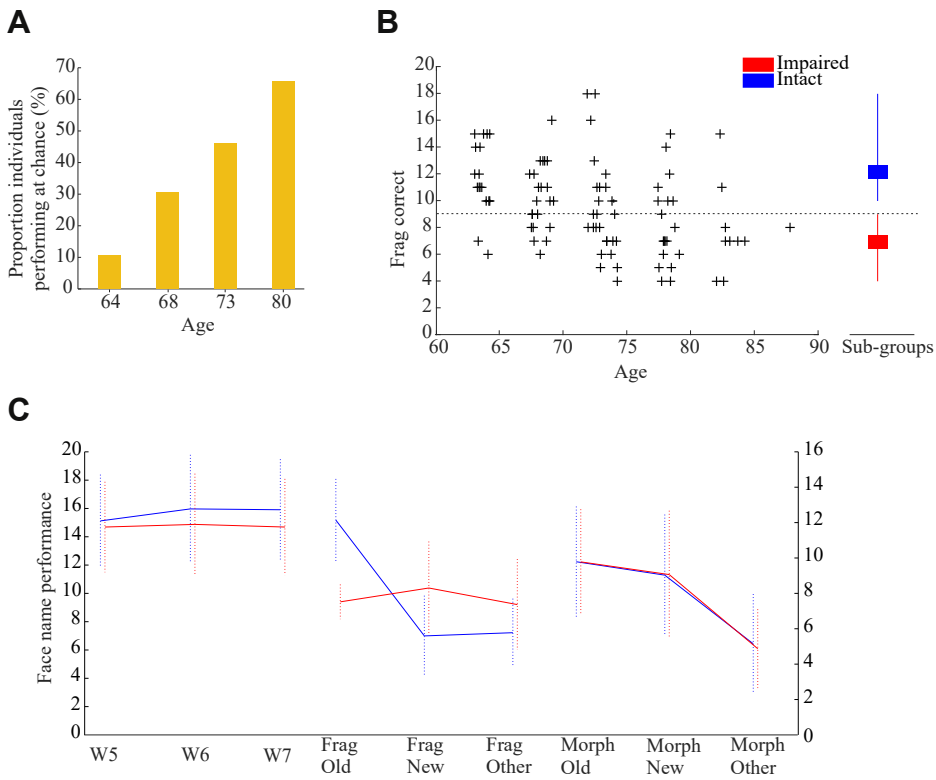


**Fig. 2.** (A) The percentage in each age group with chance performance. (B) Heterogeneity in performance on fragmented-face cues as a function of age (individuals represented by a "+"). The hatched line denotes the chance level, and the average performance and range is indicated for each sub-group on the right side. (C) Left: Mean hit rates for complete faces as a function of test wave; Middle: mean responses to fragmented faces as a function of response class; Right: mean responses to morphed faces as a function of response class. Error bars show ±1SD. Blue = intact; red = impaired.

hippocampal functional activation also for morphed face cues. In fact, the negative bars for HC and DGCA4 indicated a stronger response to new/other than old responses in the impaired group.

Finally, the longitudinal fMRI responses across Waves 5–7 during the complete face-name retrieval task were compared between the age-matched intact and impaired groups. A 2 × 3 analysis of variance was conducted. No significant group or group by time interaction in or close to the HC was found at a $p < 0.001$ (uncorrected) threshold.

### 3.3. Pattern-completion ability in relation to hippocampal-subfield volumes

Cross-sectional *FreeSurfer* analyses of structural HC data from Wave 7 provided no evidence for group differences (age-matched intact vs. impaired) in CA1 [$t(63) = 0.47$, $p = 0.64$], CA2/3 [$t(63) = 1.11$, $p = 0.27$], or DG/CA4 [$t(63) = 1.12$, $p = 0.27$] volumes. Relatedly, longitudinal analyses (see Section 2.8) revealed a significant time effect ($p < 0.001$; i.e., across Waves 5–7) but no significant effect of group or group-by-time interaction ($p$'s > 0.10) for the HC (Fig. 3D). A similar pattern as for the whole HC was observed for each subfield (Fig. 3E–G), with no group differences between the intact and impaired groups or any group by time interactions ($p$'s > 0.10).

### 3.4. Cortical volumes in relation to pattern completion

Whole-brain GM volume changes across Waves 5–7 were compared between the pattern-completion intact and impaired groups using VBM. This longitudinal VBM analysis revealed a group difference in cortical regions (Fig. 4A, upper), with the strongest effects in left parietal cortex [peak $t$-value in Brodmann area 39, $x, y, z = -46, -68, 27$; $t(63) = 4.63$] and right frontal cortex [peak $t$-value in Brodmann area 44, $x, y, z = 60, 10, 21$; $t(63) = 4.55$]. In these regions, the pattern-completion intact group displayed greater GM volume than the pattern-completion impaired group across all 3 test waves (Fig. 4A, lower panels, uncorrected $p$'s = 0.001).

### 3.5. Pattern-completion ability in relation to general cognitive function and brain volumes

From Wave 2 and onwards (i.e., across 25 years), the GCF scores in the intact group were found to be consistently higher than in the impaired group (Fig. 4B, upper panel). A group by session analysis of variance on the composite score revealed significant effects of group [$F(1,83) = 14.95$, $p < 0.001$], time [$F(5,415) = 5.89$, $p < 0.001$], and a nonsignificant interaction [$F(5,415) = 0.85$, $p = 0.52$]. The pattern was similar for both tasks that defined the GCF score (Fig. 4B, lower panels). We also analyzed data from a screening test of cognitive impairment, MMSE (Folstein et al., 1975). At Wave 2 (age range of the sample = 38–63) there was no group difference and the majority of individuals in the sample scored at or near the maximum of 30. A similar pattern was seen at Waves 3 and 4, but thereafter significant group differences were observed at Waves 5–7 (Fig. 4C). This pattern indicated emerging cognitive deficits for some individuals in the pattern-completion impaired group at the later test waves.

In continuous analyses of the entire sample ($N = 97$), a series of linear regressions were done to identify the strongest predictors of heterogeneity in pattern-completion ability (details in Table S2; all analyses included age, MMSE, and sex). First, it was found that individual differences in block design at Wave 2, when the age range of the sample was 38–63 years, predicted pattern-completion ability 25 years later (analysis 1, Table S2). Specifically, Wave 2 variability in

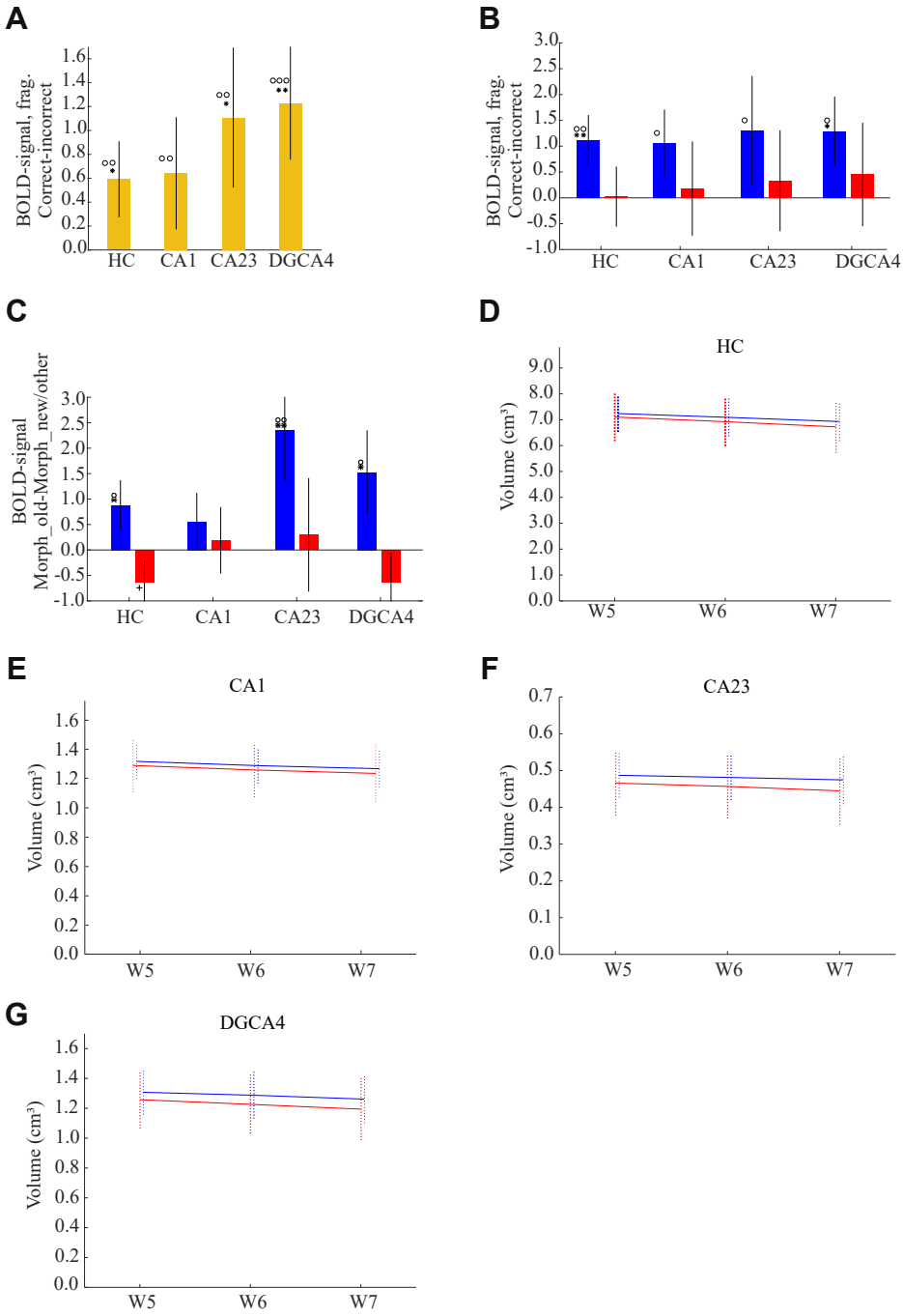


**Fig. 3.** (A) Hippocampus and hippocampal subfield responses to successful pattern completion of fragmented faces in the complete sample. (B) Hippocampus and hippocampal subfield responses to successful pattern completion of fragmented faces for the age-matched intact and impaired subgroups. (C) Hippocampus and hippocampal subfield responses to pattern completion of morphed faces (correct old > new/other) for the age-matched intact and impaired subgroups. The negative bars in the impaired group reflect a stronger response to "new/other" than "old." Circles represent *t*-tests and the stars represent the nonparametric Wilcoxon signed rank test (1 symbol: $p < 0.05$, 2 symbols: $p < 0.025$, 3 symbols: $p < 0.005$; see Table S1). Blue = intact; red = impaired. Error bars ±1 SE. (D–G) Longitudinal structural changes in the whole hippocampus (HC) and the examined subfields. Error bars show ±1 SE in (A–B) and ±1 SD in (C–F). Blue = intact; red = impaired. Key: SE, standard error.

age [$t(92) = -2.99$, $p = 0.0035$] and block design [$t(92) = 2.27$, $p = 0.026$], but not MMSE [$t(92) = 1.24$, $p = 0.22$], were significant predictors of Wave 7 performance on the fragmented-faces task.

Next, structural brain measures [HC-subfield volumes, parietal GM volume from the VBM analysis] were included in a linear regression model that examined individual differences in brain and cognitive measures at Wave 5 in relation to Wave 7 performance on the fragmented-faces task (analysis 2a, Table S2). Again, GCF was a significant predictor [$t(80) = 2.62$, $p = 0.010$], and now also MMSE [$t(80) = 4.30$, $p < 0.001$]. No brain measure from Wave 5 was a significant predictor of pattern-completion performance at Wave 7, but there was a trend for parietal GM volume [$t(80 = 1.91$, $p = 0.060$)]. When this analysis was repeated with the GCF measure separated into block design and speed scores (analysis 2b, Table S2), it was found that Block design [$t(79) = 2.52$, $p = 0.014$] but not speed [$t(79) = 0.50$, $p = 0.62$] was a significant predictor.

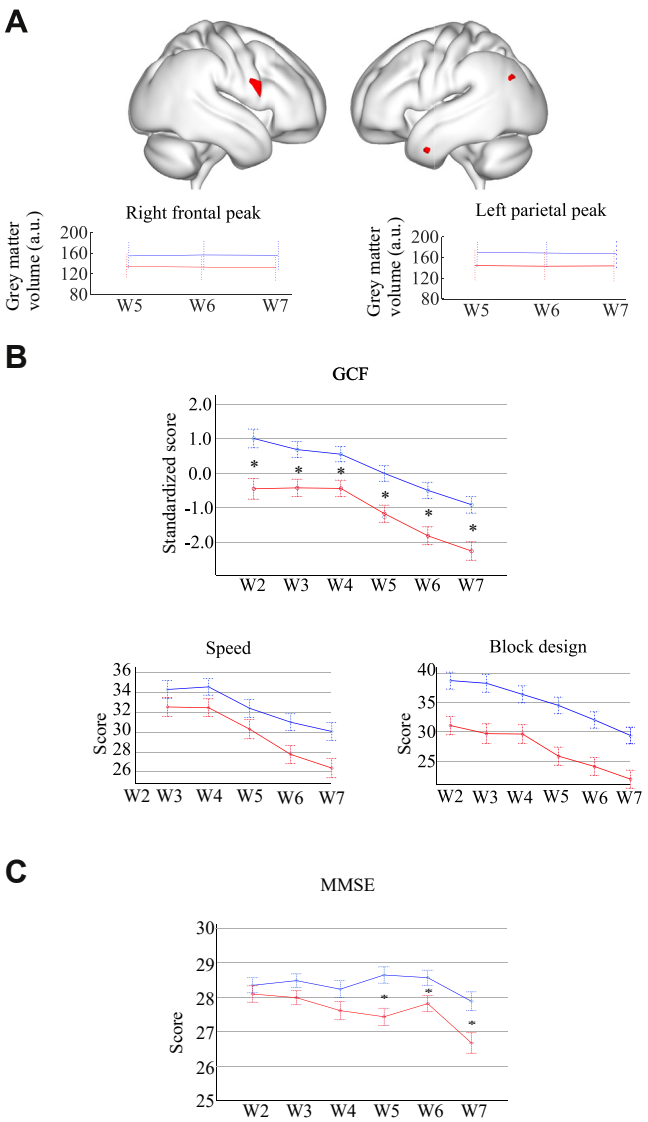


**Fig. 4.** (A) A longitudinal whole-brain VBM comparison between the intact and impaired subgroups identified peaks ($p_{uncorr}$ = 0.001) in left parietal (*x*, *y*, *z* = −46, −68, 27) and right frontal (*x*, *y*, *z* = 60, 10, 21) cortex with stable group differences across 10 years. (B) Performance of the intact and impaired groups over the 20–25 years preceding the final test wave (W7) on the composite score of general cognitive function (GCF), and the 2 subtasks that defined GCF (letter-digit and block design). (C) Mini-mental state examination (MMSE) scores as a function of group and test wave. In (B) and (C) we present age-adjusted means and error bars show ±1 SE. *Significant group differences on GCF and MMSE. Blue = intact; red = impaired. Key: SE, standard error.

A final set of linear regression models predicted Wave 7 activity in the HC and subfields from block design and MMSE at Wave 2 (analyses 3–6, Table S2) and Wave 5 cognitive and brain data (analyses 7–10 a,b, Table S2). Few significant effects were seen, with no significant relations for the overall GCF score or the speed task. However, BOLD signal variation in CA23 was predicted by block-design performance at Wave 5 [$t(79) = 2.18$, $p = 0.032$], and at trend level by block-design performance at Wave 2 [$t(84) = 1.91$, $p = 0.059$].

## 4. Discussion

We used a novel pattern-completion task to assess heterogeneity in episodic memory in aging. The results revealed that for a sizable proportion of the examined participants, the "pattern-completion impaired" group, the probability of completing fragmented face cues with the correct old names was similar to selecting new or incorrect old responses (i.e., at chance level). Despite at-chance performance on fragmented faces, the impaired group showed intact performance on complete and morphed face cues (Fig. 2C). By requiring retrieval of associated face-name pairs from elements of the pairs (Fig. 1B), all 3 face-name tasks should have taxed pattern completion to some extent. However, fragmented face cues were expected to elicit hippocampal pattern-completion processes to a higher degree than noisy cues (Hunsaker and Kesner, 2013). Therefore, these behavioral observations, combined with other recent findings (Vieweg et al., 2015, 2019), provide evidence for a pattern-completion deficit in aging.

We had predicted a specific pattern-completion response in CA3, and the fMRI analyses revealed that correctly retrieving old names based on fragmented face cues was associated with elevated BOLD signal in CA23 but also DGCA4 and CA1. Although the broader response pattern across subfields could reflect a limitation in dissecting subfields at 3T, it is in line with prior suggestions that pattern completion from degraded cues relies on an extended hippocampal circuit (Nakashiba et al., 2012)—a circuit that the pattern-completion impaired group failed to engage. Interestingly, to morphed faces, we found relatively higher hippocampal signal for new than old responses in the impaired group, whereas the pattern-completion intact group showed stronger CA3 activation for old responses (Fig. 3C). Speculatively, although a pattern-completion response (old > new/other) was elicited also by morphed faces in the intact group, the higher fMRI signal to new responses for morphed faces in the impaired group could reflect a reliance on novelty signals or other mnemonic processes. By this view, the altered fMRI response patterns in the impaired group for both fragmented and morphed cues constitute converging evidence for a pattern-completion deficit.

Analyzing factors that could explain the observed pattern-completion deficit, we first considered group differences in whole HC and subfield volumes. Both the Wave 7 cross-sectional findings and the 10-year longitudinal analysis revealed comparable volumes and patterns of atrophy in CA1, CA23, and DGCA4 in the intact and impaired groups. Atrophy was found to manifest broadly in the hippocampal region rather than in select subfields (de Flores et al., 2015). However, limited spatial resolution prevented strong conclusions in this regard, and previous studies have found stronger atrophy in the DG and CA1 regions (Adler et al., 2018). Nevertheless, the similarity in atrophy rates provided no support that differential age-related structural alterations of hippocampal subfields accounted for the deviating behavioral and hippocampal fMRI responses in the pattern-completion impaired group.

Instead, strikingly, impaired performance on the fragmented-faces task was found to map on to group differences in GCF that were stable over 25 years. In addition, in the continuous analyses, inter-individual variability in block design performance at Waves 2 and 5 was related to fragmented-faces task performance and hippocampal CA23 subfield activity up to 25 years later. Consistent with prior findings (Duncan, 2013; Jung and Haier, 2007), the intact pattern-completion group with higher GCF also displayed greater parietal cortical volumes over 10 years. Moreover, group differences in pattern-completion ability related to clinical status, as shown by a significant prediction of fragmented-faces performance by MMSE scores from Wave 5, and by a significant group difference on MMSE from Wave 5 and onwards (Small et al., 1997). Thus, individuals with higher GCF showed better preserved pattern completion in aging, were more resistant to age-related cognitive deficits, and displayed greater cortical volumes.

In pattern-completion tasks when partial/degraded cues are used to trigger episodic retrieval, such as here for fragmented faces, visuospatial processes are likely to be engaged. Such processes may be of a top-down nature, for example, to guide iterative hypothesis testing until the pattern is solved. By this view, our findings are in line with past theoretical and empirical suggestions that cortical top-down processes influence hippocampal pattern completion (Aly and Turk-Browne, 2015; Eichenbaum, 2017; Honey et al., 2017; Marr, 1971; Nyberg et al., 2019; Tang et al., 2018). Given that top-down processing decline in aging, it is not surprising that pattern completion was found to be a sensitive marker of age-related cognitive deficits. Perceptual, bottom-up processes could also influence how well individuals' complete patterns degraded faces as well as block designs. Crucially, both the top-down and bottom-up account highlight an influence of multiple processes on pattern completion and a role of many brain regions in addition to the CA23 subfield of the HC.

Our study has several strengths, notably the longitudinal nature of the Betula study design, but it also has some limitations. First, future studies should investigate longitudinal changes in pattern-completion ability in aging. Also, as we wanted to build on our face-name task that had been scanned 5 and 10 years before the final test wave, quite severe restrictions on the number of trials per category of interest had to be imposed. This restriction might have influenced aspects of the fMRI findings, but not the demonstration of a relation of pattern-completion ability with GCF. The final test wave was limited to about 100 participants. Although still relatively large for an fMRI study, in particular given longitudinal data over 10 years, the limited sample size put restrictions on the analyses we could consider as well as the statistical power. Finally, despite employment of a HR-MRI protocol, our study has limitations regarding measuring hippocampal subfields. In the longitudinal volumetric analyses, one has to be cautious in interpreting hippocampal subfield segmentation results using T1w images with a 1-mm isotropic resolution because voxel size may partially have exceeded the size of subfields (e.g., DG and CA3), and key anatomical landmarks such as the stratum radiatum lacunosum moleculare cannot be reliably identified (Adler et al., 2018). Note, though, that we found high concordance between T1w based and joint T1w and T2w based segmentations in the cross-sectional comparison.

From a more clinical point of view, while the majority of older adults adhere to an average rate of episodic-memory decline (Josefsson et al., 2012; Yaffe et al., 2009), some are more at risk than others for developing cognitive impairment and neurodegenerative diseases. The finding that pattern-completion impairment in aging mapped on to a difference in GCF (block design) 25 years earlier when there was no group difference in MMSE scores (Fig. 4B and C), provides evidence for long-term stability in brain-cognition associations (Karama et al., 2014; Walhovd et al., 2016). Thus, our observation along with related findings (Huang et al., 2018; Rantalainen et al., 2018; Whalley et al., 2000; Yaffe et al., 2009) suggest that target groups for prevention of old-age cognitive deficits can be forecasted well before older age.

## Disclosure statement

The authors have no conflicts of interest.

## CRediT authorship contribution statement

**Lars Nyberg:** Conceptualization, Methodology, Formal analysis, Writing - original draft, Writing - review & editing. **Xenia Grande:** Writing - review & editing. **Micael Andersson:** Formal analysis, Writing - review & editing. **David Berron:** Writing - review & editing. **Anders Lundquist:** Formal analysis, Writing - review & editing. **Mikael Stiernstedt:** Investigation, Formal analysis, Writing - review & editing. **Anders Fjell:** Writing - review & editing. **Kristine Walhovd:** Writing - review & editing. **Greger Orädd:** Methodology, Formal analysis, Writing - review & editing.

## Acknowledgements

This work was supported by a grant from the Knut and Alice Wallenberg (KAW) foundation, and from the European Union's Horizon 2020 program (Lifebrain; No. 732592). The FreeSurfer and ASHS segmentations were performed on resources provided by the Swedish National Infrastructure for Computing (SNIC) at HPC2N in Umeå, Sweden.

## Appendix ASupplementary data

Supplementary data to this article can be found online at https://doi.org/10.1016/j.neurobiolaging.2020.06.005.

## References

Adler, D.H., Wisse, L.E.M., Ittyerah, R., Pluta, J.B., Ding, S.-L., Xie, L., Wang, J., Kadivar, S., Robinson, J.L., Schuck, T., Trojanowski, J.Q., Grossman, M., Detre, J.A., Elliott, M.A., Toledo, J.B., Liu, W., Pickup, S., Miller, M.I., Das, S.R., Wolk, D.A., Yushkevich, P.A., 2018. Characterizing the human hippocampus in aging and Alzheimer's disease using a computational atlas derived from ex vivo MRI and histology. Proc. Natl. Acad. Sci. U. S. A. 115, 4252–4257.

Aly, M., Turk-Browne, N.B., 2015. Attention stabilizes representations in the human hippocampus. Cereb. Cortex 26, 783–796.

Arbuckle, T.Y., Maag, U., Pushkar, D., Chaikelson, J.S., 1998. Individual differences in trajectory of intellectual development over 45 years of adulthood. Psychol. Aging 13, 663–675.

Ashburner, J., 2007. A fast diffeomorphic image registration algorithm. Neuroimage 38, 95–113.

Berron, D., Vieweg, P., Hochkeppler, A., Pluta, J.B., Ding, S.-L., Maass, A., Luther, A., Xie, L., Das, S.R., Wolk, D.A., Wolbers, T., Yushkevich, P.A., Düzel, E., Wisse, L.E.M., 2017. A protocol for manual segmentation of medial temporal lobe subregions in 7 Tesla MRI. Neuroimage. Clin. 15, 466–482.

Buckner, R.L., 2004. Memory and executive function in aging and AD. Neuron 44, 195–208.

Davies, G., Armstrong, N., Bis, J.C., Bressler, J., Chouraki, V., Giddaluru, S., Hofer, E., Ibrahim-Verbaas, C.A., Kirin, M., Lahti, J., van der Lee, S.J., Le Hellard, S., Liu, T., Marioni, R.E., Oldmeadow, C., Postmus, I., Smith, A.V., Smith, J.A., Thalamuthu, A., Thomson, R., Vitart, V., Wang, J., Yu, L., Zgaga, L., Zhao, W., Boxall, R., Harris, S.E., Hill, W.D., Liewald, D.C., Luciano, M., Adams, H., Ames, D., Amin, N., Amouyel, P., Assareh, A.A., Au, R., Becker, J.T., Beiser, A., Berr, C., Bertram, L., Boerwinkle, E., Buckley, B.M., Campbell, H., Corley, J., De Jager, P.L., Dufouil, C., Eriksson, J.G., Espeseth, T., Faul, J.D., Ford, I., Scotland, G., Gottesman, R.F., Griswold, M.E., Gudnason, V., Harris, T.B., Heiss, G., Hofman, A., Holliday, E.G., Huffman, J., Kardia, S.L.R., Kochan, N., Knopman, D.S., Kwok, J.B., Lambert, J.-C., Lee, T., Li, G., Li, S.-C., Loitfelder, M., Lopez, O.L., Lundervold, A.J., Lundqvist, A., Mather, K.A., Mirza, S.S., Nyberg, L., Oostra, B.A., Palotie, A., Papenberg, G., Pattie, A., Petrovic, K., Polasek, O., Psaty, B.M., Redmond, P., Reppermund, S., Rotter, J.I., Schmidt, H., Schuur, M., Schofield, P.W., Scott, R.J., Steen, V.M., Stott, D.J., van Swieten, J.C., Taylor, K.D., Trollor, J., Trompet, S., Uitterlinden, A.G., Weinstein, G., Widen, E., Windham, B.G., Jukema, J.W., Wright, A.F., Wright, M.J., Yang, Q., Amieva, H., Attia, J.R., Bennett, D.A., Brodaty, H., de Craen, A.J.M., Hayward, C., Ikram, M.A., Lindenberger, U., Nilsson, L.-G., Porteous, D.J., Räikkönen, K., Reinvang, I., Rudan, I., Sachdev, P.S., Schmidt, R., Schofield, P.R., Srikanth, V., Starr, J.M., Turner, S.T., Weir, D.R., Wilson, J.F., van Duijn, C., Launer, L., Fitzpatrick, A.L., Seshadri, S., Mosley, T.H., Deary, I.J., 2015. Genetic contributions to variation in general cognitive function: a meta-analysis of genome-wide association studies in the CHARGE consortium (N=53 949). Mol. Psychiatry 20, 183–192.

de Flores, R., La Joie, R., Chételat, G., 2015. Structural imaging of hippocampal subfields in healthy aging and Alzheimer's disease. Neuroscience 309, 29–50.

Deary, I.J., Penke, L., Johnson, W., 2010. The neuroscience of human intelligence differences. Nat. Rev. Neurosci. 11, 201–211.

Duncan, J., 2013. The structure of cognition: attentional episodes in mind and brain. Neuron 80, 35–50.

Eichenbaum, H., 2017. Prefrontal–hippocampal interactions in episodic memory. Nat. Rev. Neurosci. 18, 547–558.

Fjell, A.M., McEvoy, L., Holland, D., Dale, A.M., Walhovd, K.B., Alzheimer's Disease Neuroimaging Initiative, 2013. Brain changes in older adults at very low risk for Alzheimer's disease. J. Neurosci. 33, 8237–8242.

Fjell, A.M., McEvoy, L., Holland, D., Dale, A.M., Walhovd, K.B., Alzheimer's Disease Neuroimaging Initiative, 2014. What is normal in normal aging? Effects of aging,

amyloid and Alzheimer's disease on the cerebral cortex and the hippocampus. Prog. Neurobiol. 117, 20–40.
Folstein, M.F., Folstein, S.E., McHugh, P.R., 1975. "Mini-mental state". A practical method for grading the cognitive state of patients for the clinician. J. Psychiatr. Res. 12, 189–198.
Gow, A.J., Johnson, W., Pattie, A., Brett, C.E., Roberts, B., Starr, J.M., Deary, I.J., 2011. Stability and change in intelligence from age 11 to ages 70, 79, and 87: the Lothian Birth Cohorts of 1921 and 1936. Psychol. Aging 26, 232–240.
Grande, X., Berron, D., Horner, A.J., Bisby, J.A., Duzel, E., Burgess, N., 2019. Holistic recollection via pattern completion involves hippocampal subfield CA3. J. Neurosci.
Honey, C.J., Newman, E.L., Schapiro, A.C., 2017. Switching between internal and external modes: a multiscale learning principle. Netw. Neurosci. 1, 339–356.
Huang, A.R., Strombotne, K.L., Horner, E.M., Lapham, S.J., 2018. Adolescent cognitive aptitudes and later-in-life Alzheimer disease and related disorders. JAMA Netw. Open 1, e181726.
Hunsaker, M.R., Kesner, R.P., 2013. The operation of pattern separation and pattern completion processes associated with different attributes or domains of memory. Neurosci. Biobehav. Rev. 37, 36–58.
Josefsson, M., de Luna, X., Pudas, S., Nilsson, L.-G., Nyberg, L., 2012. Genetic and lifestyle predictors of 15-year longitudinal change in episodic memory. J. Am. Geriatr. Soc. 60, 2308–2312.
Jung, R.E., Haier, R.J., 2007. The Parieto-Frontal Integration Theory (P-FIT) of intelligence: converging neuroimaging evidence. Behav. Brain Sci. 30, 135–154.
Karama, S., Bastin, M.E., Murray, C., Royle, N.A., Penke, L., Maniega, S.M., Gow, A.J., Corley, J., Hernández, M.V., Lewis, J.D., Rousseau, M.É., 2014. Childhood cognitive ability accounts for associations between cognitive ability and brain cortical thickness in old age. Mol. Psychiatry 19, 555–559.
Kremen, W.S., Beck, A., Elman, J.A., Gustavson, D.E., Reynolds, C.A., Tu, X.M., Sanderson-Cimino, M.E., Panizzon, M.S., Vuoksimaa, E., Toomey, R., Fennema-Notestine, C., Hagler, D.J., Fang, B., Dale, A.M., Lyons, M.J., Franz, C.E., 2019. Influence of young adult cognitive ability and additional education on later-life cognition. Proc. Natl. Acad. Sci. U. S. A. 116, 2021–2026.
Lindenberger, U., 2014. Human cognitive aging: corriger la fortune? Science 346, 572–578.
Liu, K.Y., Gould, R.L., Coulson, M.C., Ward, E.V., Howard, R.J., 2016. Tests of pattern separation and pattern completion in humans—a systematic review. Hippocampus 26, 705–717.
Marr, D., 1971. Simple memory: a theory for archicortex. Philos. Trans. R. Soc. Lond. B. Biol. Sci. 262, 23–81.
McClearn, G.E., Johansson, B., Berg, S., Pedersen, N.L., Ahern, F., Petrill, S.A., Plomin, R., 1997. Substantial genetic influence on cognitive abilities in twins 80 or more years old. Science 276, 1560–1563.
McClelland, J.L., McNaughton, B.L., O'Reilly, R.C., 1995. Why there are complementary learning systems in the hippocampus and neocortex: insights from the successes and failures of connectionist models of learning and memory. Psychol. Rev. 102, 419–457.
Nakashiba, T., Cushman, J.D., Pelkey, K.A., Renaudineau, S., Buhl, D.L., McHugh, T.J., Rodriguez Barrera, V., Chittajallu, R., Iwamoto, K.S., McBain, C.J., Fanselow, M.S., Tonegawa, S., 2012. Young dentate granule cells mediate pattern separation, whereas old granule cells facilitate pattern completion. Cell 149, 188–201.
Neunuebel, J.P., Knierim, J.J., 2014. CA3 retrieves coherent representations from degraded input: direct evidence for CA3 pattern completion and dentate gyrus pattern separation. Neuron 81, 416–427.
Nilsson, L.-G., Adolfsson, R., Bäckman, L., de Frias, C.M., Molander, B., Nyberg, L., 2004. Betula: a prospective cohort study on memory, health and aging. Aging Neuropsychol. Cogn. 11, 134–148.
Nyberg, L., Andersson, M., Lundquist, A., Salami, A., Wåhlin, A., 2019. Frontal contribution to hippocampal hyperactivity during memory encoding in aging. Front. Mol. Neurosci. 12, 229.
Nyberg, L., Lindenberger, U., 2020. Brain maintenance and cognition in old age. In: Poeppel, D., Mangun, G.R., Gazzaniga, M.S. (Eds.), Cognitive Neurosciences. The MIT Press, Cambridge.
Nyberg, L., Lövdén, M., Riklund, K., Lindenberger, U., Bäckman, L., 2012. Memory aging and brain maintenance. Trends Cogn. Sci. 16, 292–305.
Nyberg, L., Pudas, S., 2019. Successful memory aging. Annu. Rev. Psychol. 70, 219–243.
Paleja, M., Spaniol, J., 2013. Spatial pattern completion deficits in older adults. Front. Aging Neurosci. 5, 1–6.
Pudas, S., Josefsson, M., Rieckmann, A., Nyberg, L., 2018. Longitudinal evidence for increased functional response in frontal cortex for older adults with hippocampal atrophy and memory decline. Cereb. Cortex 28, 936–948.
Rantalainen, V., Lahti, J., Henriksson, M., Kajantie, E., Eriksson, J.G., Räikkönen, K., 2018. Cognitive ability in young adulthood predicts risk of early-onset dementia in Finnish men. Neurology 91, e171–e179.
Reuter, M., Schmansky, N.J., Rosas, H.D., Fischl, B., 2012. Within-subject template estimation for unbiased longitudinal image analysis. Neuroimage 61, 1402–1418.
Rönnlund, M., Sundström, A., Nilsson, L.-G., 2015. Interindividual differences in general cognitive ability from age 18 to age 65 years are extremely stable and strongly associated with working memory capacity. Intelligence 53, 59–64.
Salthouse, T.A., 2004. What and when of cognitive aging. Curr. Dir. Psychol. Sci. 13, 140–144.
Small, B.J., Viitanen, M., Bäckman, L., 1997. Mini-Mental State Examination item scores as predictors of Alzheimer's disease: incidence data from the Kungsholmen Project, Stockholm. J. Gerontol. A. Biol. Sci. Med. Sci. 52, M299–M304.
Tang, H., Schrimpf, M., Lotter, W., Moerman, C., Paredes, A., Ortega Caro, J., Hardesty, W., Cox, D., Kreiman, G., 2018. Recurrent computations for visual pattern completion. Proc. Natl. Acad. Sci. U. S. A. 115, 8835–8840.
Vieweg, P., Riemer, M., Berron, D., Wolbers, T., 2019. Memory image completion: establishing a task to behaviorally assess pattern completion in human. Hippocampus 29, 340–351.
Vieweg, P., Stangl, M., Howard, L.R., Wolbers, T., 2015. Changes in pattern completion — a key mechanism to explain age-related recognition memory deficits? Cortex 64, 343–351.
Walhovd, K.B., Krogsrud, S.K., Amlien, I.K., Bartsch, H., Bjørnerud, A., Due-Tønnessen, P., Grydeland, H., Hagler, D.J., Håberg, A.K., Kremen, W.S., Ferschmann, L., Nyberg, L., Panizzon, M.S., Rohani, D.A., Skranes, J., Storsve, A.B., Sølsnes, A.E., Tamnes, C.K., Thompson, W.K., Reuter, C., Dale, A.M., Fjell, A.M., 2016. Neurodevelopmental origins of lifespan changes in brain and cognition. Proc. Natl. Acad. Sci. U. S. A. 113, 9357–9362.
Whalley, L.J., Starr, J.M., Athawes, R., Hunter, D., Pattie, A., Deary, I.J., 2000. Childhood mental ability and dementia. Neurology 55, 1455–1459.
Yaffe, K., Fiocco, A.J., Lindquist, K., Vittinghoff, E., Simonsick, E.M., Newman, A.B., Satterfield, S., Rosano, C., Rubin, S.M., Ayonayon, H.N., Harris, T.B., Health ABC Study, 2009. Predictors of maintaining cognitive function in older adults: the Health ABC Study. Neurology 72, 2029–2035.
Yushkevich, P.A., Pluta, J.B., Wang, H., Xie, L., Ding, S.-L., Gertje, E.C., Mancuso, L., Kliot, D., Das, S.R., Wolk, D.A., 2015. Automated volumetry and regional thickness analysis of hippocampal subfields and medial temporal cortical structures in mild cognitive impairment. Hum. Brain Mapp. 36, 258–287.